Available online at www.sciencedirect.com

ScienceDirect

Scripta Materialia 89 (2014) 41–44

Scripta MATERIALIA

www.elsevier.com/locate/scriptamat

# Grain boundary depletion and migration during selective oxidation of Cr in a Ni–5Cr binary alloy exposed to high-temperature hydrogenated water

D.K. Schreiber,* M.J. Olszta and S.M. Bruemmer

*Energy and Environment Directorate, Pacific Northwest National Laboratory, Richland, WA 99352, USA*

Received 8 May 2014; revised 16 June 2014; accepted 18 June 2014
Available online 2 July 2014

High-resolution microscopy of a high-purity Ni–5Cr alloy exposed to 360 °C hydrogenated water reveals intergranular selective oxidation of Cr accompanied by local Cr depletion and diffusion-induced grain boundary migration (DIGM). The corrosion-product oxide consists of a porous, interconnected network of $Cr_2O_3$ platelets, with no further O ingress into the metal ahead. Extensive grain boundary depletion of Cr (to <0.05 at.%), typically 20–100 nm wide, is observed as a result of DIGM, and reaches depths of many micrometers beyond the oxidation front.


*Keywords:* Nickel alloys; Corrosion; Oxidation; Grain boundary diffusion; Diffusion-induced grain boundary migration (DIGM)

Intergranular (IG) corrosion and stress-corrosion cracking have been major issues for components in nuclear and other steam-based power generating systems that endure high-stress, high-temperature aqueous environments during service. Despite decades of research and the obvious connections between IG degradation and component failure [1–3], numerous questions linger about the exact mechanism by which this process occurs [4–6]. Chromium is a common alloying element in commercial Ni- and Fe-based alloys used in corrosive and oxidizing environments as it can form a protective Cr-rich surface oxide [7]. As such, the oxidation of Cr in these environments is of both practical and fundamental interest.

In this letter, the selective oxidation of Cr is studied in a model Ni–5Cr binary alloy after exposure to a simulated pressurized water reactor (PWR) primary water environment. This hydrogenated water environment is used to favor the selective oxidation of Cr over the Ni matrix. After exposure, high-resolution scanning electron microscopy (SEM), transmission electron microscopy (TEM) and atom probe tomography (APT) are employed to establish a comprehensive nanoscopic and three-dimensional picture of the intergranular oxidation process and its effects on the surrounding microstructure.

A coupon of high-purity Ni–5.4 at.% Cr binary alloy (impurity concentrations are ppm levels or less) was polished to a colloidal silica finish, suspended in a stainless steel autoclave and exposed to simulated PWR primary water (1000 appm B, 2 appm LiOH) for 1000 h at 360 °C. The dissolved hydrogen concentration was maintained at 25 cc $kg^{-1}$ (an electrochemical potential equivalent to the Ni/NiO stability line) to minimize Ni oxidation [8]. Specimens for TEM and APT analyses were extracted from the exposed coupon using standard focused ion beam lift-out and milling routines [9,10] using a FEI Helios 600 dual-beam microscope, which was also used for SEM imaging. TEM imaging was performed with a JEOL 2010F microscope at 200 kV. APT analyses were performed on a Cameca LEAP 4000X HR in laser pulsing mode ($\lambda = 355$ nm, 200 kHz repetition rate) with ~50 pJ per pulse at a base temperature of 40 K.

Representative cross-sectional SEM images of a corroded grain boundary are shown in Figure 1. The oxidized region exhibits darker contrast than the matrix and non-oxidized portion of the grain boundary. The depth of attack was assessed along 12 random, high-energy grain boundaries with an average depth of $16 \pm 7$ μm and a maximum of 33 μm. The corrosion was continuous from the exposed surface until an abrupt termination point. Limited fine voids were apparent within the oxidized regions, but there was no evidence

* Corresponding author; e-mail: daniel.schreiber@pnnl.gov

http://dx.doi.org/10.1016/j.scriptamat.2014.06.022
1359-6462/

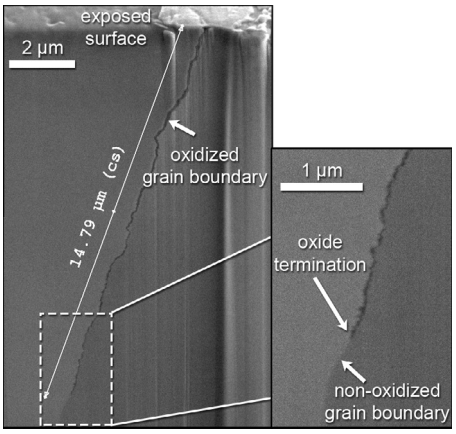


**Figure 1.** Representative cross-section SEM images of intergranular oxidation in Ni–5Cr exposed to hydrogenated water for 1000 h at 360 °C.

for voids in the metal ahead. Discrete or spatially separated oxides were not detected on any grain boundaries.

TEM analyses of the terminal region of IG oxidation are presented in Figure 2. The underfocus bright-field TEM image in Figure 2(a) confirms that the oxide is porous and that its thickness ranges from ~20 to 50 nm near the leading edge of attack. The oxides protrude from the grain boundary plane into the surrounding matrix, with no strong preference to one grain or the other. Tilting to the ⟨1 1 0⟩ zone of the top metal grain and indexing of the electron diffraction pattern in Figure 2(b) identifies the oxide as $Cr_2O_3$, which is epitaxially oriented with the metal matrix into which it protrudes. Dark-field TEM imaging of a $(0\bar{1}14)$ $Cr_2O_3$ reflection reveals individual oxide platelets that are ~5 nm thick and ~20–50 nm long. STEM energy-dispersive X-ray spectroscopy (EDS) mapping of the grain boundary region surrounding the oxide termination shown in Figure 2(c) illustrates the significant composition variations for O, Cr and Ni. The O signal is constant along the oxidized region and terminates abruptly, revealing no discrete oxide precipitates beyond the oxidation front. Chromium is enriched in the oxide, while Ni is strongly depleted. Ahead of the oxidation front, Cr is depleted to low levels (~1.4 at.% by EDS) at leading grain boundaries with concomitant Ni enrichment. The slight increase in brightness of the Ni signal within the Cr-depleted zone could suggest Ni diffusion ahead of the oxidation front, but it is not clear whether this contrast is real or possibly an artifact from preferential ion milling during sample preparation. The width of the Cr-depleted zone varies from ~25 to 70 nm, with the most extensive depletion adjacent to the oxidation front. Significant Cr depletion was apparent along grain boundaries to depths of >3 μm beyond the oxidation front in this sample and reached depths of ~10 μm along other attacked boundaries.

The position of the grain boundaries, readily apparent within the STEM bright-field image, has been superimposed onto the Cr EDS map as yellow dashed lines. With this overlay, it is apparent that the Cr depletion occurs exclusively to one side of the grain boundary plane. This asymmetry indicates that the Cr depletion is not the result of matrix diffusion of Cr into the grain boundary plane but instead indicates that diffusion-induced grain boundary migration (DIGM) has occurred [11]. Chromium diffuses rapidly to the oxidation front along the grain boundary plane, causing the grain boundary to migrate preferentially into one grain, leaving in its wake a Cr-depleted, Ni-rich zone. This Cr depletion is also apparent on one side of the IG oxide, proving that the grain boundary had migrated and formed the Cr-depleted zone prior to oxidation. Similar DIGM was observed in identically exposed Ni–4Al samples described previously [12], but the migration is much more extensive for Ni–5Cr than for Ni–4Al, both in width and distance ahead of the oxidation front.

APT analyses ahead of the IG oxidation front were used to quantify the Cr depletion as a function of depth. Three APT specimens were prepared and analyzed from a single grain boundary, though not the same grain boundary as shown by TEM in Figure 2. A separate APT specimen was also prepared at a grain boundary ~500 μm into the specimen to determine the bulk grain boundary composition and revealed no significant Cr enrichment or depletion (Fig. S1). Figure 3(a) depicts elemental atom maps ~100 nm ahead of the oxidation front, and 2 at.% Cr isoconcentration surfaces (orange ribbons) are used to outline the Cr-depleted zone. Close inspection of the Ni map reveals variations in the local atomic density as a result of the crystal symmetry of each grain, highlighted by the regions labeled *i* and *ii* for grains 1 and 2, respectively. The symmetry of grain 1 clearly terminates at its intersection with the 2 at.% Cr isoconcentration, indicated by a red X. This indicates a change in crystal symmetry and the presence of a grain boundary. Conversely, the crystal symmetry observed in grain 2 extends across the Cr isoconcentration surface and into the Cr-depleted zone. Therefore the Cr-depleted zone has the same crystal orientation as grain 2. This relatively rough and diffuse interface represents the approximate position of the grain boundary before DIGM occurred. Concentration profiles from APT analyses are displayed in Figure 3(b). Within 100 nm of the oxidation front (top profile), Cr is observed to be totally depleted (to <0.05 at.%) from a region ~15 nm wide before gradually returning to the nominal 5 at.% Cr concentration. The relatively sharp interface to the left of the grain boundary shows that minimal matrix diffusion has occurred to replace the depleted Cr. Approximately 2 μm beyond the oxidation front (middle profile), Cr is depleted to ~0.9 at.% at the grain boundary plane (<5 nm width) and rises from ~4 at.% to its nominal matrix value across ~20 nm. The relatively diffuse interface with the left grain demonstrates significant matrix diffusion of Cr, indicating that this region of the grain boundary is not rapidly migrating. A profile extracted ~9 μm ahead of the oxidation front (bottom profile) shows similar depletion to ~0.9 at.% Cr across a broad region (~85 nm wide), before returning abruptly to the nominal Cr concentration. The relatively sharp interface with the left grain indicates that minimal matrix Cr diffusion into the grain boundary plane has occurred. The detected concentration of O is also plotted in all three profiles. Within experimental error (<0.01 at.%), no O was detected in any of these profiles.

From these combined analyses, it is clear that selective IG oxidation of Cr has occurred during exposure